IRWIN AND JOAN JACOBS
CENTER FOR COMMUNICATION AND INFORMATION TECHNOLOGIES

Absorption enhancement by matching the cross-section of plasmonic nanowires to the field structure of tightly focused beams

Alexander Normatov, Boris Spektor, Yehuda Leviatan, and Joseph Shamir

CCIT Report #784
February 2011

DEPARTMENT OF ELECTRICAL ENGINEERING
TECHNION - ISRAEL INSTITUTE OF TECHNOLOGY, HAIFA 32000, ISRAEL

CCIT Report #784 February 2011

Absorption enhancement by matching the cross-section of plasmonic nanowires to the field structure of tightly focused beams

Alexander Normatov,[1,*] Boris Spektor,[1] Yehuda Leviatan,[1] and Joseph Shamir[1]

[1]*Department of Electrical Engineering, Technion – Israel Institute of Technology, Technion City, Haifa 32000, Israel*
[*]*alexn@tx.technion.ac.il*

Abstract: Localized surface plasmon resonance is characterized by a significant electric field component normal to some parts the surface. Shaping the surface to be normal to the direction of an incident electric field may increase the incident power coupling to the excited plasmonic mode, enhancing the absorption in lossy nanowires. In this work we perform a numerical analysis to investigate the dependence of the absorption on the shape of the nanowire cross-section for two cases of tightly focused beam illumination. We show that nanowires occupying a relatively small portion of the beam waist area can still absorb up to 65% of the power of the incident beam.

Keywords: Scattering, particles; Surface plasmons.

References and links

1. S. A. Maier, *Plasmonics: Fundamentals and Applications* (Springer 2007).
2. K. Li, M. I. Stockman, and D. J. Bergman, "Self-Similar Chain of Metal Nanospheres as an Efficient Nanolens," Phys. Rev. Lett. **91**, 227402 (2003).
3. S. E. Sburlan, L. A. Blanco, and M. Nieto-Vesperinas, "Plasmon excitation in sets of nanoscale cylinders and spheres," Phys. Rev. B **73**, 035403 (2006).
4. V. A. Podolskiy, A. K. Sarychev, E. E. Narimanov, and V. M. Shalaev, "Resonant light interaction with plasmonic nanowire systems," J. Opt. A: Pure Appl. Opt. **7,** S32–S37 (2005).
5. J. P. Kottmann and O. J. F. Martin, "Plasmon resonances of silver nanowires with a nonregular cross section," Phys. Rev. B **64**, 235402 (2001).
6. J. P. Kottmann and O. J. F. Martin, "Plasmon resonant coupling in metallic nanowires," Opt. Express **8**, 655-663 (2001).
7. M. Gu, and X. Li, "The Road to Multi-Dimensional Bit-by-Bit Optical Data Storage," Optics & Photonics News **21**, 28-33 (2010).
8. C. J. R. Sheppard, "High-aperture beams," J. Opt. Soc. Am. A **18**, 1579-1587 (2001).
9. K. S. Youngworth and T. G. Brown, "Focusing of high numerical aperture cylindrical vector beams," Opt. Express **7**, 77-87 (2000).
10. A. Normatov, B. Spektor and J. Shamir, "High numerical aperture focusing of singular beams," Proc. SPIE **7277**, 727709 (2009).
11. C. Rockstuhl and H. P. Herzig, "Wavelength-dependent optical force on elliptical silver cylinders at plasmon resonance," Opt. Lett. **29**, 2181-2183 (2004).
12. J. Lerme, G. Bachelier, P. Billaud, C. Bonnet, M. Broyer, E. Cottancin, S. Marhaba and M. Pellarin, "Optical response of a single spherical particle in a tightly focused light beam: application to the spatial modulation spectroscopy technique," J. Opt. Soc. Am. A **25**, 493-514 (2008).
13. K. Sendur, W. Challener and O. Mryasov, "Interaction of spherical nanoparticles with a highly focused beam of light," Opt. Express **16**, 2874-2886 (2008).
14. N. M. Mojarad, G. Zumofen, V. Sandoghdar and M. Agio, "Metal nanoparticles in strongly confined beams: transmission, reflection and absorption," J. Europ. Opt. Soc. Rap. Public. **4**, 09014 (2009).
15. M. Dienerowitz, M. Mazilu, P. J. Reece, T. F. Krauss and K. Dholakia, "Optical vortex trap for resonant confinement of metal nanoparticles," Opt. Express **16**, 4991-4999 (2008).
16. K. C. Toussaint, Jr., M. Liu, M. Pelton, J. Pesic, M. J. Guffey, P. Guyot-Sionnest, and N. F. Scherer, "Plasmon resonance-based optical trapping of single and multiple Au nanoparticles," Opt. Express **15**, 12017 -12029 (2007).
17. J. J. Stamnes, "Focusing of two-dimensional waves," J. Opt. Soc. Am. **71**, 15–31 (1981).
18. J. J. Stamnes and H. A. Eide, "Exact and approximate solutions for focusing of two-dimensional waves. I. Theory," J. Opt. Soc. Am. A **15**, 1285-1291 (1998).

19. A. Normatov, B. Spektor and J. Shamir, "The quadratic phase factor of tightly focused wavefronts," Opt. Comm. **283**, 3585-3590 (2010).
20. A. Normatov, B. Spektor and J. Shamir, "Tight focusing of wavefronts with piecewise quasi-constant phase," Opt. Eng. **48**, 028001 (2009).
21. Y. Leviatan and A. Boag, "Analysis of Electromagnetic Scattering from Dielectric Cylinders Using a Multifilament Current Model," IEEE Trans. Antennas and Propagation **AP-35**, 1119-1127 (1987).
22. Y. Leviatan, Am. Boag and Al. Boag, "Analysis of TE Scattering from Dielectric Cylinders Using a Multifilament Magnetic Current Model," IEEE Trans. Antennas and Propagation **AP-36**, 1026-1031 (1988).
23. Y. Leviatan, Am. Boag, and Al. Boag, "Generalized Formulations for Electromagnetic Scattering from Perfectly Conducting and Homogeneous Material Bodies-Theory and Numerical Solution," IEEE Trans. Antennas and Propagation **AP-36**, 1722-1734 (1988).
24. U. Kreibig, "Electronic properties of small silver particles: the optical constants and their temperature dependence," J. Phys. F: Met. Phys. **4**, 999-1014 (1974).
25. X. W. Chen, V. Sandoghdar and Mario Agio, "Nanofocusing radially-polarized beams for high-throughput funneling of optical energy to the near field," Opt. Express **18**, 10878-10887 (2010).
26. B. S. Luk'yanchuk, and V. Ternovsky, "Light scattering by a thin wire with a surface-plasmon resonance: Bifurcations of the Poynting vector field," Phys. Rev. B **73**, 235432 (2006).
27. M. V. Bashevoy, V. A. Fedotov and N. I. Zheludev, "Optical whirlpool on an absorbing metallic nanoparticle," Opt. Express **13**, 8372-8379 (2005).

1. Introduction

Localized surface plasmon resonance (SPR) in sub-wavelength metal nanoparticles can be excited by direct illumination [1]. The SPR can dramatically increase the fields inside the particle and in the near zone outside the particle, especially when a set of such particles is considered [2]. Similar behavior can be observed for finite length cylinders [3, 4] and for 2D cylinder structures and sets [5, 6]. Stronger fields inside lossy materials mean enhanced power absorption. The localized heating effect can be useful in applications like biology. The plane wave incident illumination, as in the examples above, may not be suitable in applications requiring higher illumination localization or higher absolute incident power. For example, optical data storage applications [7] use the tightly focused illumination.

The field structure of tightly focused beams contains features having spatial dimensions smaller than the wavelength, especially when beams containing singularities are considered [8-10]. Recently, there was a growing interest in interaction between nano-particles or nano-cylinders and tightly focused beams [11-14] as well as in trapping of metal particles by focused beams under plasmon resonance conditions [15, 16].

In this work we seek to enhance the absorption of a tightly focused beam by a silver nanowire. While other works studied given objects under given illumination, we study the absorption of a given illumination by an object adapted to that illumination. We suggest a technique for the initial shaping of the nanowire cross-section based on the analysis of the tightly focused field. Then, we investigate the absorption as a function of the geometric feature size of the cross-section of various nanowire shapes.

The next section presents the technique and its application to the two selected beams. Section 3 discusses the various geometric features and the corresponding absorption results. The evaluation of the near field and the power flow for a selected case is presented in section 4, which is followed by conclusions.

2. Defining the object shape

"*Localized surface plasmons … are non-propagating excitations of the conduction electrons of metallic nanostructures coupled to the electromagnetic field*" [1]. Ideally, maximizing the coupling would require matching all the components of the surrounding field to the SPR mode of the given nanostructure. In our problem, we are presented with a given *incident* field and we attempt to find the nanostructure shape that maximizes the coupling, and consequently the absorption. Modifications of the nanostructure shape affect its resonant mode and its *scattered* field which in turn changes the *total* field, being the sum of the *incident* and the *scattered* fields. Thus, for the sake of simplicity, we choose the *incident* field for determination of our initial shape guess. The other simplification is based on the fact that the concentrations of free

charges at some portions of the nanostructure surface are related to the locally normal electric field component. This field component is used as a predictor of the degree of coupling between the surrounding field and the SPR mode.

The above can be summarized in the following technique. Consider a 2D geometry, which is uniform along the *y* axis. The nanowire is represented by an infinite cylinder parallel to the *y* axis. The nanowire cross-section is shaped in a way that maximizes the normal incident electric field on its circumference. Denoting the incident field by $\bar{E}_{inc} = \hat{x}E_{inc,x} + \hat{z}E_{inc,z}$, the circumference of the nanowire cylinder by $C(x,z)$ and the total circumference length by C_{tot}, we look for shapes maximizing a parameter *M*, defined by the relation,

$$M = \max\left\{\left[\oint_{C(x,z)} \left|\hat{n}\cdot\bar{E}_{inc}\right| dC\right] \Big/ C_{tot}\right\}, \qquad (1)$$

where $\hat{n}$ is a unit normal to the nanowire circumference. After the initial nanowire cross-section shape is defined, its parameters can be varied for maximizing the absorption, as will be described later.

Application of the above technique requires rigorous evaluation of the incident field components, as a function of position, in the vicinity of the geometric focus of a focusing system. The optical system is schematically illustrated in Fig. 1. An incident plane wave, polarized in the *x* direction, propagates along the *z* axis. At the entrance pupil of a focusing optical system it passes a phase mask, which will be discussed later. As indicated earlier, the discussion is restricted to a 2D geometry, assuming that along the *y* axis the problem is uniform and infinite; the tightly focused field is formed in the vicinity of the geometric focal line *O*, parallel to the *y* axis. The rigorous evaluation of the 2D focused field can be performed using either Kirchhoff or Debye boundary conditions [17-19]. These boundary conditions partly depend on the phase mask located at the entrance pupil. When this phase mask is uniform across the pupil, the result corresponds to the tightly focused plane wave (PW). When this phase mask is a π step function, the result corresponds to the tightly focused dark beam (DB) [20].

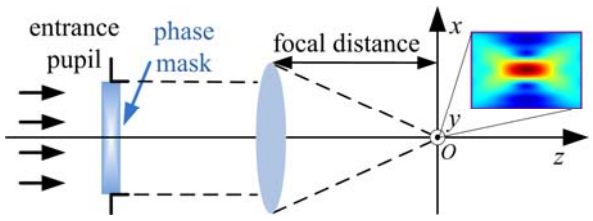

Fig. 1. Optical system schematic. The inset shows the electric field amplitude of the tightly focused plane wave in the *xz* plane.

The amplitude value of the electric field of the tightly focused PW is shown in Fig. 2(a) as a normalized color-code. As the polarization is not strictly linear through the focused field, visualizing the direction of the electric field is not trivial. Instead, we define here the inclination of the incident field as:

$$\alpha = -sign(z)\tan^{-1}\left(\left|E_{inc,x}(x,z)\right| \Big/ \left|E_{inc,z}(x,z)\right|\right). \quad (2)$$

The field inclination is visualized by the short white lines. Applying the above technique, one can suggest the axial plate nanowire cross-section shape shown cyan. Under the PW illumination, the calculated value of *M* in (1) is normalized to about 100 in arbitrary units (a.u.). As a comparison, for the cylinder cross-section, shown green, the value of *M* is between 70 and 40 a.u. depending on the cylinder diameter as shown in Fig. 3(a). The two other cross-sections shown black and magenta will be suggested for the DB illumination. Under the PW illumination their *M* values are 80 to 40 a.u. and 50 to 30 a.u. respectively.

The tightly focused field of a DB with the same nanowire cross-sections outlined is shown in Fig. 2(b). The field structure in this case is more complicated due to the presence of an optical singularity. Two cross-section shapes can be suggested here. First, similarly to the former case, two plates can be placed along the beam direction as outlined by black. The value of *M* is about 70 a.u. for the two-plate structure. Another suggested cross-section shape is a plate oriented along the lateral x axis as outlined in magenta. For this case the value of *M* is between 55 and 40 a.u. depending on the object dimensions as indicated in Fig. 3(b). Under the DB illumination the *M* value of the axial plate cross-section, shown cyan is 30 to 20 a.u., and for the cylinder cross-section it is 60 to 45 a.u..

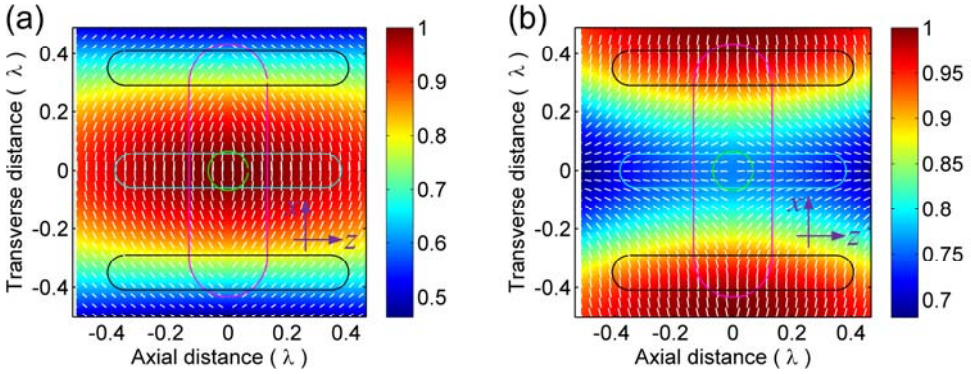

Fig. 2. The electric field of the tightly focused PW (a), the tightly focused DB (b) and the chosen nanowire cross-section shapes. The amplitude value is color-coded and normalized independently. The field inclination is shown white.

3. Matching shapes for absorption enhancement

Having defined the initial cross-section shapes for the two illumination cases, we proceed with matching of the shapes for absorption maximization. The absorption is measured as the integral on the net power flowing into the volume, containing the investigated structure. The volume is defined as a cylinder, centered on the geometrical focal line *O* having radius equal to the optical system focal distance. The power is calculated for the *total* field, following the evaluation of the *scattered* field by the source model technique [21-23]. In this work we are concerned with silver nanowires having dielectric constant $\varepsilon_{Ag} = -1.07 + 0.29i$ under the illumination wavelength of $\lambda = 338nm$. It must be noted that the dielectric constant value is close to that of the circular cylinder electrostatic resonance. The effects of heating of the material and the resulting change of its optical properties are not accounted for. The dimensions of the investigated silver nanowires are considered large enough to neglect the dependence of the imaginary part of ε_{Ag} on the cylinder size [24].

Nanowire cross-section shape matching is performed by varying some geometrical parameters of the shape and calculating power absorption for each parameter value. For comparison, the absorption of all the shapes is calculated for both illuminations as shown in Fig. 3 as a function of the corresponding geometrical feature size. In case of the axial plate, shown cyan, the only varied parameter is plate length, while its width is fixed on 0.118λ (40nm). For the two parallel plates the varied parameters are the distance between them (plain black line) and their lengths (black plus marks). Their width is fixed 0.118λ (40nm), when the distance is varied, the length is constant 0.7λ (237 nm) and when the length is varied, the distance is constant 0.7λ (237 nm). The results of the varied distance between plates exclude a range where there is an overlap between locations of sources used by the source model technique. The lateral plate has its length varied (plain magenta line) and its width varied (magenta plus marks). The chosen constant values for the lateral plate were: width = 0.27λ (90nm), length 0.6λ (203nm). The absorption results for the changing diameter of the circular cylinder are shown green. The chosen constant values correspond to the shapes in Fig. 2.

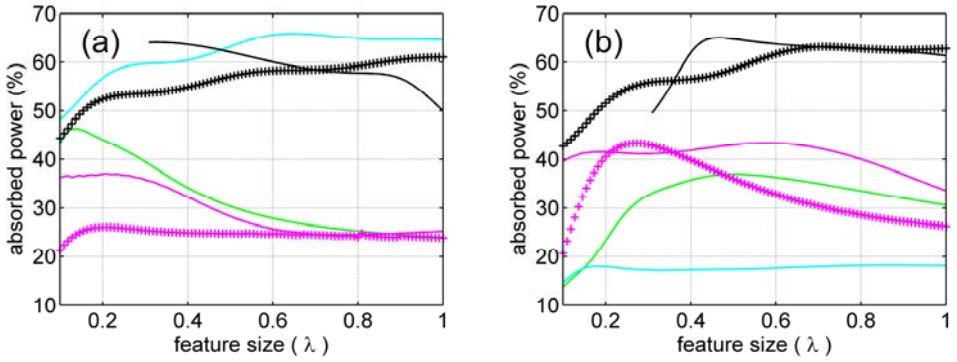

Fig. 3 The plot of absorption, as a function of nanowire cross-section shape parameters for the tightly focused PW (a), and for the tightly focused DB (b).

The absorption results under the tightly focused PW illumination are shown in Fig. 3(a). The axial plate shows best absorption topping at about 65%. It is closely followed by the parallel plates. The cylinder with the circular cross section shows a relatively high absorption, above 40%, reaching its peak for the diameter of 0.136λ. With increasing size, it scatters more and absorbs less. It is interesting to note that a similar absorption value was reported for metal spheres in tightly focused beams [14]. For the cylinder diameters close to the width of the axial plate, the absorption results are similar to those of very short plates. The laterally oriented plate shows smaller absorption, as it may be expected from the relatively low *M* values. These results indicate, as expected, that shapes having higher *M* values tend to have higher absorption and vice versa.

The absorption results for the tightly focused DB illumination are shown in Fig. 3(b). The parallel plates show the best absorption here for a wide range of feature sizes, topping at about 65%. The lateral plate shows absorption above 40%. The shape of the lateral plate, from the view point of matching to the incident field, bears some resemblance to the surface plasmon polariton excitation in a nanowire in [25], where the maximum coupling efficiency was reported to be above 90%. For the cylinder, the highest absorption value of about 35% is reached for cylinder diameter of about λ/2, which is where the cylinder approaches the major streams of the power flow. The axial plate shows relatively low absorption, regardless of its length, as it is situated in the singularity region. In case of the tightly focused DB illumination, the prediction of absorption by *M* is less accurate although still relevant.

4. Near field results and power flow

It is interesting to assess the field and the power flow in the vicinity of the highly absorbing nanowire. Fig. 4(a) shows the total electric field for the case of the axial plate shaped for maximum absorption. The apparent differences with the incident field are field enhancement at the left tip of the plate, and the inclination of the total electric field along the plate sides, which is no longer nearly normal but it makes almost 45° with the surface. The vertical axis on Fig. 4(a) is shifted down to accommodate the inset showing the overall near field distribution. Interference of the reflected wave with the incident wave can be observed in the inset.

The change in the electric field inclination means that the power crosses the object boundary and flows into the plate. The distribution of the power flow in the vicinity of the plate is shown in Fig. 4(b). The plate is positioned as in Fig. 4(a) and includes the inset zooming on the power flow distribution at the plate tip oriented towards the incident wave (the left tip). It can be observed that the power flow distribution pattern is not trivial. The power flow crosses the sides of the plate, flows inside the plate towards the left tip and forms a number of whirlpools and bifurcations in that area. Partly, the power flows into the plate through the leftmost tip. At the zone where the tip interfaces the sides of the plate, the power flows out of the plate. It is comforting to note that the Poynting vector distribution and its

topological features have a number of notable similarities to the results presented in Refs. [26, 27].

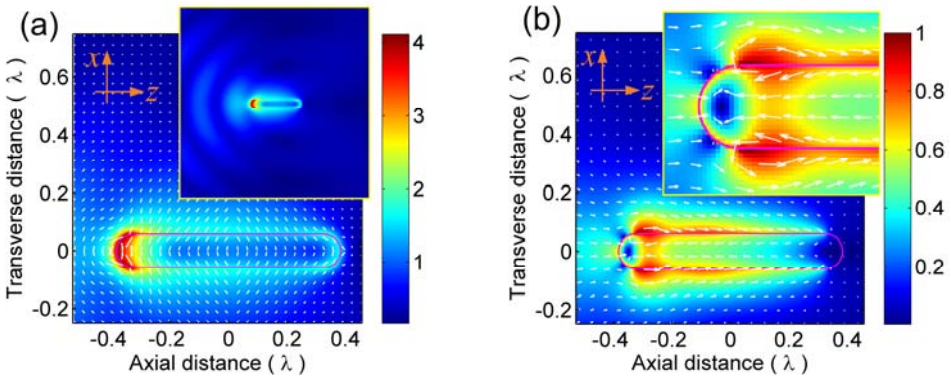

Fig. 4. The electric field (a) normalized with the same value as Fig. 2(a) and the Poynting vector (b) corresponding to the matched plate in the focused PW. The insets show (a) the zoom out at the whole waist area, (b) the zoom in on the power flow near the tip of the plate.

The color-scale of Fig. 4(b) suggests that the power flow in the vicinity and inside the plate has a significantly higher magnitude than in free space away from the plate. Thus the overall beam power flow (from left to right) is not apparent from the figure, although it still exists.

5. Outlook and conclusions

The above results show that the suggested approach for nanowire cross-section adjustment allows enhancing the absorption up to 65% of the power of an incident tightly focused beam. It is remarkable that properly shaped absorbing nanowires, sized below the classical resolution limit, induce such significant changes in an incident beam. The suggested technique for the initial shape guess proved itself capable of achieving high absorption results in spite of the simplifications made.

Straight forward application of our approach may be useful for devising absorbing bodies intended to heat themselves or their surroundings. The approach has a potential to be extended to the design of structures for efficient coupling of tightly focused beams into SPPs. Considering the impact of the enhanced absorption on the far field, the approach can be used in metrology and positioning applications.

Acknowledgments

This work was partially supported by a grant from the Center for Absorption in Science of the Ministry of Immigrant Absorption and the Committee for Planning and budgeting of the Council for Higher Education under the framework of the KAMEA Program.